AAC Journals.ASM.org

Population Modeling and Simulation Study of the Pharmacokinetics and Antituberculosis Pharmacodynamics of Isoniazid in Lungs

L. Lalande,[a] L. Bourguignon,[a,b] S. Bihari,[c] P. Maire,[a,b] M. Neely,[d] R. Jelliffe,[d] S. Goutelle[a,b,e]

Université Lyon 1, UMR CNRS 5558, Biométrie et Biologie Evolutive, Villeurbanne, France[a]; Hospices Civils de Lyon, Hôpital P. Garraud, Service Pharmaceutique, Lyon, France[b]; Department of Critical Care Medicine, Flinders Medical Centre and Flinders University, Bedford Park, South Australia, Australia[c]; Laboratory of Applied Pharmacokinetics, University of Southern California, Children's Hospital of Los Angeles, Los Angeles, California, USA[d]; Université Lyon 1, Faculté de Pharmacie, Lyon, France[e]

Among first-line antituberculosis drugs, isoniazid (INH) displays the greatest early bactericidal activity (EBA) and is key to reducing contagiousness in treated patients. The pulmonary pharmacokinetics and pharmacodynamics of INH have not been fully characterized with modeling and simulation approaches. INH concentrations measured in plasma, epithelial lining fluid, and alveolar cells for 89 patients, including fast acetylators (FAs) and slow acetylators (SAs), were modeled by use of population pharmacokinetic modeling. Then the model was used to simulate the EBA of INH in lungs and to investigate the influences of INH dose, acetylator status, and *M. tuberculosis* MIC on this effect. A three-compartment model adequately described INH concentrations in plasma and lungs. With an MIC of 0.0625 mg/liter, simulations showed that the mean bactericidal effect of a standard 300-mg daily dose of INH was only 11% lower for FA subjects than for SA subjects and that dose increases had little influence on the effects in either FA or SA subjects. With an MIC value of 1 mg/liter, the mean bactericidal effect associated with a 300-mg daily dose of INH in SA subjects was 41% greater than that in FA subjects. With the same MIC, increasing the daily INH dose from 300 mg to 450 mg resulted in a 22% increase in FA subjects. These results suggest that patients infected with *M. tuberculosis* with low-level resistance, especially FA patients, may benefit from higher INH doses, while dose adjustment for acetylator status has no significant impact on the EBA in patients with low-MIC strains.

Despite the introduction of "short-course chemotherapy" of tuberculosis (TB) 40 years ago, TB remains one of the leading causes of death in the world. According to the World Health Organization (WHO), tuberculosis was still responsible for 1.7% of all human deaths in 2012 (1).

First-line anti-TB agents include rifampin, isoniazid (INH), pyrazinamide, and ethambutol. As no new first-line anti-TB drug has been developed for 50 years, there is a need for anti-TB treatment optimization. In addition to poor patient compliance and drug resistance, low concentrations of anti-TB drugs may negatively affect treatment outcomes (2). Low plasma levels have been associated with longer times to respond to treatment, treatment failure, and the emergence of drug resistance (3–5).

Among the first-line anti-TB treatments, INH kills the largest proportion of fast-growing *Mycobacterium tuberculosis* in lungs over the first 2 to 5 days of therapy (6, 7). As a result, INH displays the greatest early bactericidal activity (EBA) among all anti-TB drugs, with EBA being the average decline in *M. tuberculosis* counts in sputum during the first 2 days of therapy (8). Due to its great initial bactericidal activity, INH is key to reducing contagiousness among treated patients. INH microbial kill rates decrease greatly after 2 to 5 days of therapy. It has been hypothesized that this decline in INH activity is due to depletion of bacilli in the exponential phase of growth (9). Another hypothesis explaining the biphasic kill curve for INH is the emergence of INH-resistant bacilli (10).

In humans, INH is metabolized mainly by *N*-acetyltransferase 2 (NAT-2). This enzyme displays a genetic polymorphism, with fast (F) and slow (S) alleles. Although three genotypes are possible (FF, FS, and SS), it is often difficult to distinguish homozygotic FF and heterozygotic FS fast acetylators (FAs) without genetic data (11). Most pharmacokinetic (PK) studies consider only two acetylator phenotypes, i.e., fast acetylators, for whom elimination half-lives range from 0.9 to 1.8 h, and slow acetylators (SAs), for whom elimination half-lives range from 2.2 to 4.4 h (12). As a consequence, when they are treated with the same INH dose, fast acetylators display lower INH concentrations, area under the concentration-time curve (AUC) values, and EBAs than do slow acetylators.

The pharmacokinetic (PK)-pharmacodynamic (PD) index that best explains microbial killing by INH is the AUC/MIC ratio (13, 14). This PK-PD relationship was specifically studied in a mouse model of tuberculosis, in which INH plasma AUC values were correlated with the decline in the total bacterial load in lungs (13), and in a hollow-fiber *in vitro* model, in which the AUC values were correlated with the decline in log counts, which probably reflects the *in vivo* effect of INH on extracellular bacteria (14). In humans, INH AUC values have also been shown to correlate with EBA values (15).

INH pharmacokinetics have been extensively studied in plasma but not in lungs, and no model describing the time course

Received 24 February 2015 **Returned for modification** 16 April 2015
Accepted 30 May 2015

Accepted manuscript posted online 15 June 2015

Citation Lalande L, Bourguignon L, Bihari S, Maire P, Neely M, Jelliffe R, Goutelle S. 2015. Population modeling and simulation study of the pharmacokinetics and antituberculosis pharmacodynamics of isoniazid in lungs. Antimicrob Agents Chemother 59:5181–5189. doi:10.1128/AAC.00462-15.

Address correspondence to L. Lalande, laure.lalande@chu-lyon.fr, or S. Goutelle, sylvain.goutelle@chu-lyon.fr.

doi:10.1128/AAC.00462-15

of INH exposure in lungs is available. As the concentrations in lungs are thought to drive the effects of anti-infective agents in pulmonary infections (16), it is desirable to quantify the relationships between INH doses, concentrations, and effects in the lungs. The aims of this study were to develop a pulmonary INH pharmacokinetic model and to explore the relationships between INH pharmacokinetics and antimicrobial effects against *M. tuberculosis* in lungs by use of simulations.

MATERIALS AND METHODS

Patient population and data collection. This was a retrospective analysis of primary pharmacokinetic data from three original studies published by Conte et al., O'Brien et al., and Katiyar et al. (17–19). Details about subjects' characteristics, informed consent, and study design are fully available in those publications (17–19). Briefly, the study by Conte et al. (17) included 80 adult volunteers without TB, i.e., 20 men with AIDS, 20 men without AIDS, 20 women with AIDS, and 20 women without AIDS. In each subgroup, one-half of the subjects had a fast acetylator phenotype for INH metabolism, and the other one-half had slow acetylator status. Caffeine was used to determine acetylator status (20). All subjects received 300 mg of INH, administered orally, once a day for 5 days. INH concentrations were measured in plasma prior to administration of the first dose and then 1 h and 4 h after administration of the last directly observed dose. INH concentrations in epithelial lining fluid (ELF) and alveolar cells (AC) recovered by bronchoalveolar lavage (BAL) were measured approximately 4 h after administration of the last dose. All sampling times were recorded precisely for each individual. INH concentrations were measured by high-performance liquid chromatography, as described elsewhere (21). For the determination of INH concentrations in ELF and AC, the volume of ELF recovered by BAL was calculated by using the urea dilution method (22), while the volume of AC was estimated from the cell count performed on the BAL fluid. The study by O'Brien et al. (18) included 6 patients with active pulmonary TB, i.e., 1 woman with AIDS, 2 men without AIDS, and 3 men with unknown AIDS status. These subjects received 300 mg of INH, administered orally, once a day as part of a four-drug therapeutic regimen, for a minimum of 5 days. Approximately 2 h after the dose, INH concentrations were measured in plasma and in ELF recovered by BAL. INH concentrations were measured by high-performance liquid chromatography (23), and the volume of ELF recovered by BAL was calculated by using the urea dilution method. The study by Katiyar et al. (19) included 6 healthy volunteers who received a single oral dose of 250 mg of INH in association with rifampin and pyrazinamide. INH concentrations were measured in plasma prior to administration and then 1 h, 2 h, 4 h, and 24 h after INH administration. INH concentrations in the BAL fluid were also determined in the original study; they were not included in our analysis, however, because the volume of BAL fluid recovered was not known and so the concentrations in ELF and AC could not be determined. Available covariates included TB status for all subjects, age and sex for 83 of 92 subjects, HIV status for 80 subjects, and weight, height, creatinine clearance, and INH acetylator status for 80 subjects. For quantitative covariates (e.g., body weight and age), missing values were fixed to the median. The HIV status was assumed to be negative when not known. For the acetylator status, preliminary runs were performed with Monolix software and a mixture model was used to allocate status for subjects for whom it was not known, based on their measured concentrations.

Population pharmacokinetic modeling. Population pharmacokinetic analyses were carried out with two different algorithms. The initial analysis was performed with a parametric method, namely, the stochastic approximation expectation maximization (SAEM) method implemented in Monolix software (version 4.3.2; Lixoft, Orsay, France). It was used to identify the best structural model and to perform the covariate analysis. The nonparametric adaptive grid (NPAG) algorithm implemented in Pmetrics software was used for the final analysis and simulation studies, because this program has shown its ability to identify outliers (24, 25). The initial steps were performed with Monolix software to reduce the computation time.

In the initial analysis performed with the SAEM method, INH concentrations in plasma, ELF, and AC were modeled simultaneously. A diagonal covariance model and a combined error model (additive and proportional) were set. We assumed log-normal distribution for all parameters. The best structural pharmacokinetic model was a three-compartment model consisting of plasma, ELF, and AC plus an oral depot compartment, with first-order elimination and first-order processes for all transfer constants. Because INH oral bioavailability could not be estimated, it was fixed to 1. The absorption rate constant was also fixed, based on literature data (12). A covariate analysis was performed using a forward stepwise-backward deletion method. The criterion for model selection was based on the objective function value (OFV) (OFV = $-2 \times$ log likelihood).

The final structural model obtained with the SAEM method was implemented in the NPAG algorithm. The influence of acetylator status on INH elimination was introduced into the model as a linear relationship. The model was described by the following system of ordinary differential equations:

$$dX_a/dt = -k_a \cdot X_a \quad (1)$$

$$dX_1/dt = k_a \cdot X_a - k_e \cdot X_1 - k_{12} \cdot X_1 + k_{21} \cdot X_2 \quad (2)$$

$$dX_2/dt = k_{12} \cdot X_1 - k_{21} \cdot X_2 - k_{23} \cdot X_2 + k_{32} \cdot X_3 \quad (3)$$

$$dX_3/dt = k_{23} \cdot X_2 - k_{32} \cdot X_3 \quad (4)$$

$$k_e = k_i + \mathrm{AS} \cdot k_s \quad (5)$$

where X_a, X_1, X_2, and X_3 (all in milligrams) are the amounts of drug in the absorption compartment, the central compartment (plasma concentrations), the ELF compartment, and the AC compartment, respectively, k_a (in hours^{-1}) is the absorption rate constant, k_e (in hours^{-1}) is the elimination rate constant from the central compartment and is a function of the acetylator status (AS), AS is a binary variable whose value is equal to 0 for slow acetylators and 1 for fast acetylators, and k_{12}, k_{21}, k_{23}, and k_{32} (in hours^{-1}) are the between-compartment transfer rate constants. The other pharmacokinetic parameters are the three volumes of distribution from the following output equations:

$$Y_1 = X_1/V_{\mathrm{plasma}} \quad (6)$$

$$Y_2 = X_2/V_{\mathrm{ELF}} \quad (7)$$

$$Y_3 = X_3/V_{\mathrm{AC}} \quad (8)$$

where Y_1, Y_2, and Y_3 (in milligrams per liter) are the INH concentrations in the central compartment, the ELF compartment, and the AC compartment, respectively; V_{plasma} represents the volume of distribution in the central compartment, V_{ELF} that in the ELF compartment, and V_{AC} that in the AC compartment (all in liters).

In the NPAG modeling procedure, each drug concentration was weighted by the reciprocal of the assay variance at that concentration. The overall assay pattern was determined from the assay validation published by Delahunty et al. (21), by fitting a second-order polynomial to the plot of the assay standard deviation (SD) versus the mean concentration (x). The resulting equations for the plasma, ELF, and AC INH concentrations were as follows:

$$\mathrm{SD}_{\mathrm{plasma}} = 0.0075 + 0.0391x + 0.0017x^2 \quad (9)$$

$$\mathrm{SD}_{\mathrm{ELF}} = 0.0175 + 0.1423x + 0.0006x^2 \quad (10)$$

$$\mathrm{SD}_{\mathrm{AC}} = 0.0175 + 0.0733x + 0.0006x^2 \quad (11)$$

In the NPAG algorithm, the equation of the assay error is multiplied by a coefficient denoted gamma, which is estimated by the NPAG algorithm and accounts for other clinical sources of error.

Individual predicted concentrations were computed by using the median of each patient's individual Bayesian posterior parameter joint density. Goodness of fit was assessed by the objective function value and by regression analysis of predicted versus observed concentrations. Bias (de-

TABLE 1 Population characteristics

Characteristic	Value
Age (mean ± SD) (yr)	36.7 ± 8.5
Weight (mean ± SD) (kg)	70 ± 13
Height (mean ± SD) (cm)	169 ± 10
No. male/no. female/no. of unknown sex	43/40/6
Creatinine clearance (mean ± SD) (ml/min)	105 ± 26
No. of slow acetylators/no. of fast acetylators/no. with unknown acetylator status	39/38/12
No. HIV positive/no. HIV negative/no. with unknown HIV status	41/39/9
No. with TB/no. without TB	6/83

fined as the mean error of prediction), precision (defined as the root mean square error of prediction), and visual examination of residuals were used to assess predictive performance.

Monte Carlo simulations. The Pmetrics simulator was used to perform several 1,000-subject Monte Carlo simulations. The simulation from the nonparametric prior distribution was performed in a semiparametric way. In this method, each population support point (i.e., each parameter set in the discrete collection) is used as the mean of a normal distribution within a larger multimodal multivariate distribution (26). In order to avoid extreme and unrealistic pharmacokinetic parameters, parameter limits that were specified in the model file were also used for the simulations. Each simulated parameter set that contained a parameter value outside the defined range was ignored, and another set was generated. Each 1,000-subject simulation was performed for both fast and slow acetylators. The mean, median, and standard deviation (SD) of the simulated PK parameters were similar to those estimated by the NPAG algorithm in the population analysis (data not shown).

The 24-h concentration-time profiles for INH in plasma, ELF, and AC were calculated for each subject, after the administration of two oral doses of INH. Simulations of longer INH therapy were not performed because the effects of INH need to be maximized over the very first days of therapy. Four dosing regimens of INH were evaluated, i.e., the standard daily dose of 300 mg and higher daily doses of 450 mg, 600 mg, and 900 mg. In order to assess the pharmacodynamic effects of INH against *M. tuberculosis* in this simulated population, the ratios of the AUC from time zero to 24 h (AUC_{0-24}) (in mg · h/liter) to the MIC were computed for plasma, ELF, and AC concentrations for all subjects. Eight INH MICs for *M. tuberculosis* (0.015625, 0.03125, 0.0625, 0.125, 0.25, 0.5, 1, and 2 mg/liter) were considered in the calculations of the AUC_{0-24}/MIC ratios (27, 28). Matlab software (version 8.2; The MathWorks, Natick, MA) was used for AUC calculations and postprocessing of results.

We then calculated the predicted microbial killing of *M. tuberculosis* in lungs corresponding to each ELF AUC_{0-24}/MIC ratio, using the equation determined in the *in vitro* hollow-fiber model from Gumbo et al. (14), at day 3 of treatment. We assumed that this model best reflected the initial bactericidal effects of INH against extracellular bacilli in the ELF. The log decline in *M. tuberculosis* density (effect) (in $\log_{10}$ CFU per milliliter per day) was calculated as follows:

$$\text{Effect} = \left([2.89 \times (AUC_{0-24}/MIC)^{0.9}] / [(AUC_{0-24}/MIC)^{0.9} + 61.55^{0.9}]\right)/3 \quad (12)$$

This equation is a Hill equation, also known as a sigmoidal E_{max} model, where 2.89 $\log_{10}$ CFU/ml is the maximal decline (i.e., the maximal effect [E_{max}]), 61.55 is the AUC_{0-24}/MIC ratio associated with 50% of maximal killing (median effect exposure), and the exponent 0.9 is the coefficient of sigmoidicity. Because the original equation from Gumbo et al. (14) described the total microbial killing by INH over 3 days, the predicted effect was divided by 3 to estimate an average daily effect. These simulations were performed for the four INH dosage regimens and the 8 MIC values described above, for 1,000 slow and 1,000 fast acetylators, in order to assess the influences of INH dose size, *M. tuberculosis* MIC, and acetylator status on the initial bactericidal effects of INH in the lungs.

RESULTS

Pharmacokinetic modeling. Data from 89 of 92 subjects were used in the analysis. Three subjects from the study by Conte et al. (17) were excluded because they had undetectable INH plasma concentrations at all sampling times. Two of them were male, and the third was female; all three were HIV negative. The characteristics of the 89 subjects are presented in Table 1.

The three-compartment model estimated with the SAEM method provided acceptable fit (results not shown). The only covariate that significantly improved the model fit was the acetylator status, which was found to influence the INH plasma elimination rate constant, as expected. This parameter-covariate relationship was associated with a 46.3-point decrease in the objective function.

The NPAG analysis yielded a joint parameter distribution of 72 discrete support points. The population parameter values estimated with the use of the NPAG algorithm are summarized in Table 2. The gamma coefficient of the residual error model (see equation 3) was estimated as 2.96. The absorption rate constant value was fixed according to literature findings (12) because data in the absorption phase were too sparse to yield reliable estimates for this population.

Predicted concentrations based on the median Bayesian posterior parameter estimates correlated well with the observed concentrations (Fig. 1), although some outliers (high concentrations in the ELF and AC) could not be captured by the model. The bias and precision of the Bayesian posterior predictions from the NPAG analysis were acceptable (Table 3).

The individual estimates of INH AUC_{0-24} in plasma, ELF, and AC after the first dose, as provided by the NPAG analysis, are summarized in Table 4. The mean AUC_{0-24} values were greater for SA subjects than for FA subjects for plasma and ELF but surpris-

TABLE 2 Summary statistics for population PK parameters estimated with NPAG algorithm[a]

Parameter	k_a (h^{-1})	k_i (h^{-1})	k_s (h^{-1})	k_{12} (h^{-1})	k_{21} (h^{-1})	k_{23} (h^{-1})	k_{32} (h^{-1})	V_{plasma} (liters)	V_{ELF} (liters)	V_{AC} (liters)
Mean	2.57	1.372	0.800	9.584	9.899	9.266	11.276	51.3	49.9	53.7
SD		1.364	0.693	6.468	6.869	7.772	7.820	44.5	46.0	42.0
Median		0.761	0.712	9.250	9.860	7.435	11.334	22.7	30.3	39.7
25th percentile		0.353	0.136	3.593	3.731	0.572	2.738	12.7	10.7	14.2
75th percentile		1.808	1.380	14.160	16.466	17.852	19.718	102.6	117.2	95.4

[a] The k_a value was fixed from literature data. The elimination rate constant (k_e) for slow acetylators is equal to k_i. The elimination rate constant for fast acetylators is equal to $k_i + k_s$ (mean, 2.172 h^{-1}).

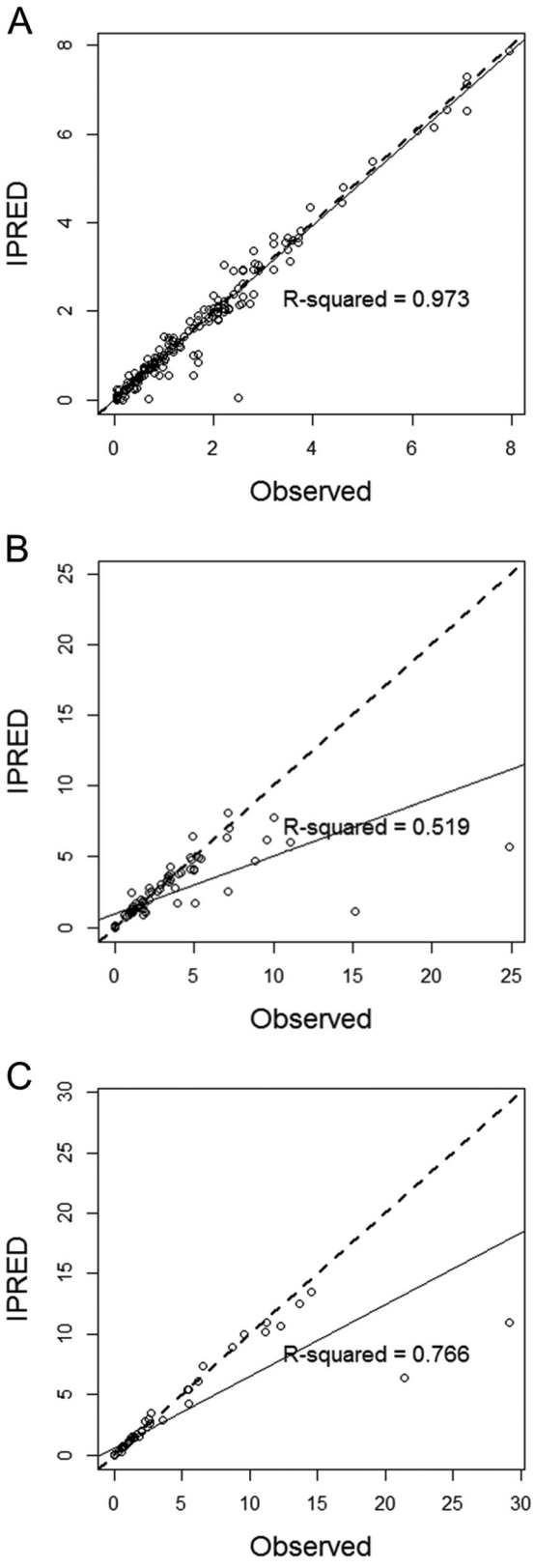

FIG 1 Plots of observed INH concentrations versus individual median Bayesian posterior predictions (IPRED) for plasma (A), ELF (B), and AC (C). Solid lines, best regression lines; dashed lines, identity lines. Concentrations are expressed in milligrams per liter.

TABLE 3 Predictive performance of Bayesian posterior concentration estimates obtained with NPAG algorithm

Compartment	Bias[a] (mg/liter)	Precision[b] (mg/liter)
Plasma	−0.14	1.17
ELF	0.76	3.77
AC	−1.18	5.24

[a] Calculated as the mean error of prediction.
[b] Calculated as the root mean square error of prediction.

ingly not AC. It is noteworthy that the variability in the AUC_{0-24} values for the two lung compartments was very large, with some subjects having very low or undetectable INH concentrations.

Monte Carlo simulations. Twenty-four-hour simulated profiles of median INH concentrations in plasma, ELF, and AC after the second oral administration of the 300-mg INH dose, for slow and fast acetylators, are depicted in Fig. 2. INH exposure in lungs (ELF and AC) was systematically greater than that in plasma. Also, INH exposure in the three compartments was greater for slow acetylators than for fast acetylators, as expected.

Plots of the predicted daily decline in *M. tuberculosis* density as a function of the MIC with various INH doses for fast and slow acetylators are displayed in Fig. 3 and Fig. 4, respectively. First, we observed that the predicted effects declined markedly with increasing MICs. Actually, the results showed that the influences of INH dose and acetylator status on INH effects were strongly dependent on *M. tuberculosis* susceptibility. Also, for each MIC, there was large overlap in the effects associated with the four simulated doses. With a low MIC of 0.0625 mg/liter, which has been the value observed most frequently for clinical isolates (27), increases in the daily dose from 300 mg to 450 mg and 600 mg were associated with increases in the mean daily killing in FA subjects of only 7 and 11%, respectively. Indeed, the daily *M. tuberculosis* kill values were 0.71 ± 0.19 $\log_{10}$ CFU/ml/day with 300 mg INH, 0.76 ± 0.18 $\log_{10}$ CFU/ml/day with 450 mg INH, and 0.79 ± 0.17 $\log_{10}$ CFU/ml/day with 600 mg INH. The mean bactericidal effects of the 300-mg dose of INH were increased by only 11% in SA subjects, compared with FA subjects (decline of 0.71 ± 0.19 $\log_{10}$ CFU/ml/day in FA subjects versus 0.79 ± 0.18 $\log_{10}$ CFU/ml/day in SA subjects).

With a higher *M. tuberculosis* MIC value of 1 mg/liter (defined as the concentration for high-level clinical resistance [29]), however, increases in the daily dose of INH from 300 mg to 450 mg and 600 mg for FA subjects resulted in larger increases in the mean bactericidal effect, i.e., 22% and 41%, respectively. Indeed, the daily *M. tuberculosis* kill values were 0.27 ± 0.18 $\log_{10}$ CFU/ml/day with 300 mg INH, 0.33 ± 0.20 $\log_{10}$ CFU/ml/day with 450 mg INH, and 0.38 ± 0.21 $\log_{10}$ CFU/ml/day with 600 mg INH. With the 300-mg dose of INH and the same MIC of 1 mg/liter, SA

TABLE 4 Individual plasma, ELF, and AC AUC_{0-24} estimates after first INH dose for 89 subjects

Compartment	AUC_{0-24} (mean ± SD) (mg · h/liter)		
	All subjects (n = 89)	SA subjects (n = 39)	FA subjects (n = 38)
Plasma	11.3 ± 8.6	11.7 ± 7.7	7.3 ± 6.3
ELF	24.5 ± 25.2	27.6 ± 22.3	18.8 ± 26.0
AC	23.8 ± 38.3	15.7 ± 27.8	29.8 ± 41.0

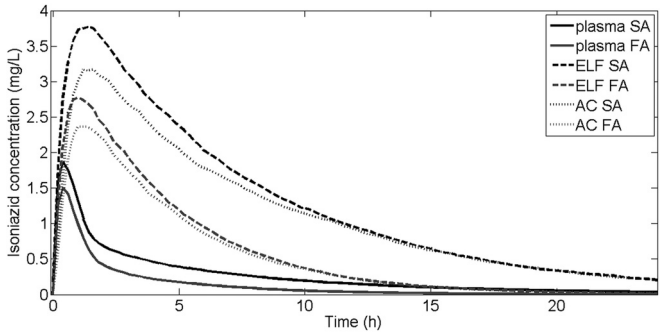

FIG 2 Time profiles of median INH concentrations in plasma, ELF, and AC after the second oral 300-mg dose of INH. AC, alveolar cells; ELF, epithelial lining fluid; FA, fast acetylator; SA, slow acetylator.

individuals had 41% greater mean bactericidal effects than FA subjects (decline of 0.27 ± 0.18 $\log_{10}$ CFU/ml/day in FA subjects versus 0.38 ± 0.22 $\log_{10}$ CFU/ml/day in SA subjects). Indeed, doubling the INH dose from 300 mg to 600 mg in FA subjects yielded bactericidal effects similar to those observed in SA subjects with the standard 300-mg dose (mean of 0.38 $\log_{10}$ CFU/ml/day). With a *M. tuberculosis* MIC of 1 mg/liter, however, even if the dose was increased to 900 mg per day, the mean bactericidal effect was much lower than that associated with the standard 300-mg dose against *M. tuberculosis* with an MIC of 0.0625 mg/liter or lower.

DISCUSSION

We used population pharmacokinetic modeling to describe the pulmonary exposure to INH in a group of 89 subjects who were originally included in three different studies. A three-compartment linear model with an oral depot compartment, including INH acetylator status as a covariate influencing INH elimination, adequately described the data. This three-compartment, 10-parameter model was the simplest structure for describing the three-output system.

The influence of acetylator status on INH pharmacokinetics was expected and is in accordance with previous pharmacokinetic studies that described a major effect of NAT-2 genotype or acetylator phenotype on INH clearance (30–32). The population pharmacokinetic parameter estimates in our study were broadly consistent with previously published results except for the INH elimination rate constant (k_e), which appeared large for both fast and slow acetylators, compared with estimates by Peloquin et al. (12, 33). Initially our results might appear unrealistic, because half-lives, which are usually calculated as log(2) divided by k_e, would be much lower than the usual ranges, which are about 1 to 2 h and 2 to 4.5 h for FA and SA subjects, respectively (12). In the two studies by Peloquin et al. (12, 33), the INH elimination rate constant was estimated from a one-compartment model, in which the basic calculation applies. The concept of half-life is different when a multicompartment model is used, however, as in our analysis, and various calculation methods have been proposed (34, 35). A universal way to calculate half-life is to consider a continuous intravenous infusion of the drug and to calculate the time to reach the steady-state plateau concentration. About 97% and 99% of the plateau concentration is reached after 5 and 7 half-lives, respectively. When we simulated a continuous intravenous infusion of INH using our three-compartment model and the median parameter values shown in Table 2, the INH half-life, calculated as one-fifth of the time to reach 97% of the plateau concentration, was 2.44 h for SA subjects and 1.30 h for FA subjects. These values are in agreement with the usual values calculated from one-compartment models.

The mean AUC_{0-24} values estimated for the 89 individuals were also consistent with published results (12, 33, 36, 37), but very large variabilities in INH exposure were observed in both plasma and lungs. Among the 89 subjects included in the analysis, 77 of 89 subjects were included in the study by Conte et al. (17). In that study, a significant number of concentrations were not detectable in plasma and ELF. In our analysis, 15 of 166 INH plasma concentrations were below the limit of quantification, as were 22

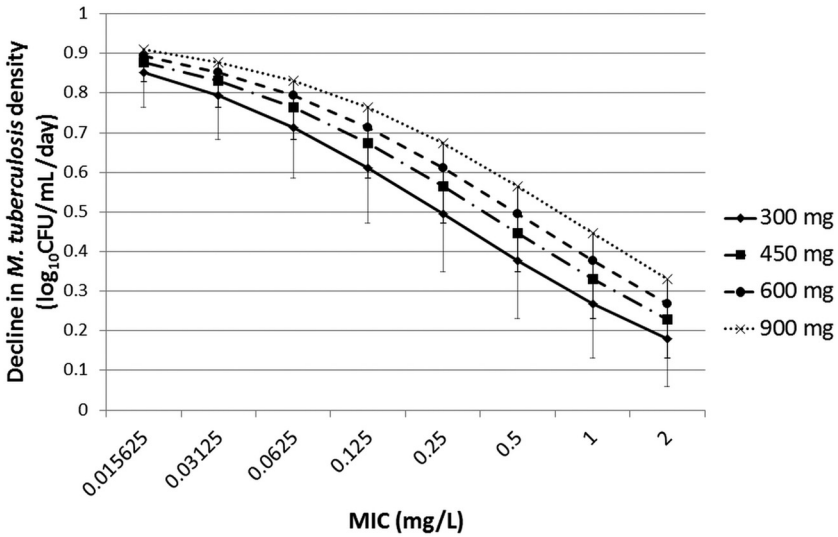

FIG 3 Simulated decline in *M. tuberculosis* density in the ELF in fast acetylator subjects as a function of *M. tuberculosis* MIC and INH dose. Each curve represents the daily decline (mean ± standard deviation) for each INH dose. Vertical bars, standard deviations. For ease of graphical display, the standard deviations are shown only for the INH doses of 450 and 900 mg.

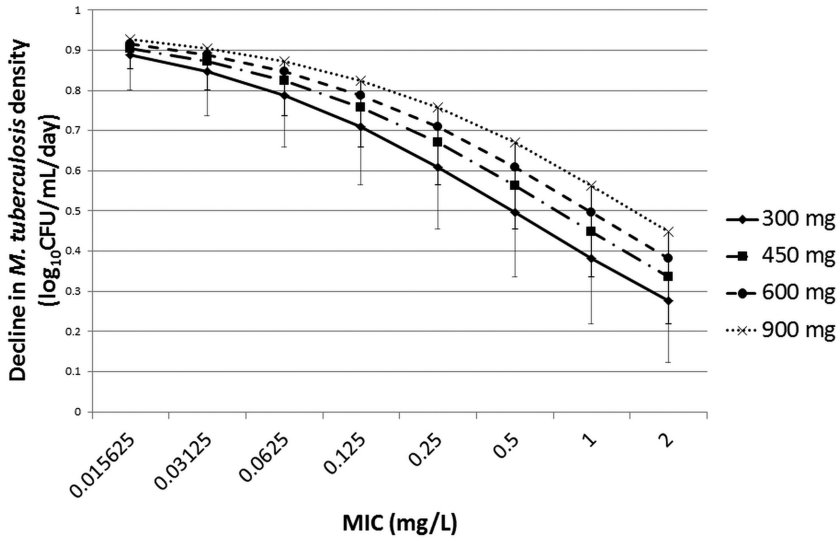

FIG 4 Simulated decline in *M. tuberculosis* density in the ELF in slow acetylator subjects as a function of *M. tuberculosis* MIC and INH dose. Each curve represents the daily decline (mean ± standard deviation) for each INH dose. Vertical bars, standard deviations. For ease of graphical display, the standard deviations are shown only for the INH doses of 450 and 900 mg.

of 89 ELF concentrations. All such concentrations originated from the study by Conte et al. (17). Because the last dose before measurement was taken under direct supervision, patient compliance cannot be questioned in that study. The reason for such low INH exposure levels in that specific study remains unclear.

INH is a cornerstone of the current standard chemotherapy for TB. It is a potent bactericidal drug against fast-growing susceptible TB bacilli and is thought to provide most of the antibacterial effect over the first 2 to 5 days for multidrug therapy. The acetylator status is a major determinant of INH exposure. However, the need for INH dose optimization and adjustment for acetylator status is controversial. Clinical studies that assessed the EBA values with various doses of INH found that the EBA seems to plateau at 300 mg daily, as no significant increase in the EBA was observed with larger INH doses (6, 15, 38). However, it was shown that the EBA of INH in fast acetylators was significantly lower than that in slow acetylators (15). A simulation study by Gumbo et al. suggested that a 300-mg daily dose of INH may be suboptimal, especially in ethnic populations with large proportions of FA individuals (14). However, that article did not report the simulated effects of higher INH doses. Also, a recent meta-analysis of clinical studies reported that microbiological failure, relapse, and acquired drug resistance were observed more frequently for fast acetylator subjects than for slow acetylator subjects (39). However, it is noteworthy that most studies included in this meta-analysis evaluated isoniazid-containing regimens that are no longer in use today. Indeed, there was no study on the first-line short-course chemotherapy currently recommended by the World Health Organization.

The aim of our simulations was to evaluate the early decline of *M. tuberculosis* in the ELF, in SA and FA subjects, with various INH doses. With the standard 300-mg daily dose of INH, the mean daily declines in *M. tuberculosis* density in the ELF were 0.79 and 0.71 $\log_{10}$ CFU/ml/day for SA and FA individuals, respectively, with an MIC of 0.0625 mg/liter, which is the most common MIC for *M. tuberculosis* clinical isolates (27). These values for declines in *M. tuberculosis* density, although at the upper end of the range, are consistent with average EBA values reported in clinical studies, which ranged from 0.37 to 1.0 $\log_{10}$ CFU/ml/day (40, 41). Therefore, the antibacterial effects of INH in the ELF predicted by the model appear consistent with the early clinical effects of the drug.

Our simulations indicated that, with the standard daily dose of 300 mg, even though SA subjects always exhibit greater bactericidal effects in the ELF than FA subjects, the difference is small as long as the MIC of *M. tuberculosis* remains low (0.125 mg/liter or less). In accordance with this finding, increasing the daily INH dose up to 600 mg gave little increase in bactericidal effects, even in FA subjects, when the MIC was at the lower end of the MIC range. Those results are in accordance with clinical studies that found no increase in the EBA when the INH dose was increased beyond 150 to 300 mg per day (6, 15, 38). While those studies did not report the MICs of isolated strains of *M. tuberculosis*, we may hypothesize that those MICs were relatively low.

Gumbo et al. previously performed a PK-PD simulation of the EBA as a function of INH doses and acetylator proportions (14). The results of their simulations in a population with 88% fast acetylators may be compared to our results for a group with 100% FA individuals. The mean EBA values predicted by Gumbo et al. (14) (numbers obtained by digitalization of the plot) were about 0.81, 0.61, and 0.32 $\log_{10}$ CFU/ml/day for MIC values of 0.016, 0.064, and 0.256 mg/liter, respectively. We predicted mean EBA values of 0.85, 0.71, and 0.50 $\log_{10}$ CFU/ml/day for FA subjects with similar MIC values (0.015625, 0.0625, and 0.25 mg/liter, respectively). Therefore, our results appear consistent with those reported by Gumbo et al. (14) for low MICs, but the decline in the effects with increasing MIC values was less in our study. This may be due to the difference in the concentrations used to drive the effects in the models. Gumbo et al. (14) assumed that the effect was driven by INH plasma concentrations, while the effect was linked to ELF concentrations in our simulations. Because ELF concentrations were greater, on average, than plasma concentrations in our study, so were the associated effects.

Gumbo et al. also showed that the average EBA may fall to a suboptimal level (about 0.3 $\log_{10}$ CFU/ml/day) at the upper end of the MIC range, especially for FA subjects (14). However, those authors did not assess the effects of higher INH doses. Our results suggest that the benefits of increasing the INH dose may be significant only if patients are infected with *M. tuberculosis* strains with relatively high MICs. For example, a 20% increase in the mean EBA in FA subjects can be achieved with a dose increase from 300 mg to 600 mg only if the MIC is greater than 0.125 mg/liter. In other words, with MICs greater than 0.125 mg/liter, the EBA values for FA and SA subjects become substantially different. It is interesting to note that this MIC value has been suggested by Gumbo et al. as a new susceptibility breakpoint, based on patients' clinical responses (42).

For patients with sensitive strains with low MICs, our simulations showed that any dose increase would have little influence on the EBA, even for FA subjects. The reason for this lies in the exposure-effect curves for INH identified by Jayaram et al. and Gumbo et al. (13, 14). The bactericidal effects of INH appeared to plateau for AUC_{0-24}/MIC ratios of about 250 to 500. Such ratios are well achieved in most patients with standard INH doses, provided that the MIC is low.

Currently, the WHO recommends an INH dose of 5 mg/kg (range, 4 to 6 mg/kg) for all patients, irrespective of acetylator status. Some published studies have suggested individualizing INH dosages according to the acetylator genotype, to yield similar drug exposures and EBA values; homozygous fast acetylators would require higher doses (6 to 7.5 mg/kg), whereas lower doses of 2.5 to 3 mg/kg would be sufficient for homozygous SA subjects (30, 32). As low and high INH resistance levels have been defined on the basis of MICs of $\geq$0.2 mg/liter and $\geq$1 mg/liter, respectively (29), our results suggest that high doses of INH may be most useful for patients infected with low-level drug-resistant *M. tuberculosis*, especially FA subjects. Little clinical information on such use of higher doses of INH exists. The WHO considers high-dose INH therapy (16 to 20 mg/kg) a treatment option for multidrug-resistant tuberculosis (43). Although the role of such treatment is denoted as "unclear" by the WHO, it has been shown to achieve earlier and persistent sputum clearance and the best radiological improvement (44). There may be concerns about the tolerability of such higher doses, as some data indicate that INH neurotoxicity and hepatotoxicity may increase with increasing drug exposure (45, 46). Further research is required to clarify the potential benefits and risks of high-dose INH treatment.

This study has several limitations that should be considered. First, only 6 of 89 subjects were infected with *M. tuberculosis*. The pulmonary PK of INH may be altered in TB patients because of lung lesions (47). A study with a large number of TB patients would be necessary to address potential differences from healthy subjects. Also, while HIV infection was not found to influence INH PK in this study, the number of subjects with HIV ($n = 41$) and PK data, especially for the absorption phase, were insufficient for thorough investigation of this issue.

Second, the simulation part of the study required several underlying assumptions. We used the relationship between AUC/MIC and microbial killing in lungs established by Gumbo et al. (14). Those authors used a hollow-fiber system in which *M. tuberculosis* cultures were placed in contact with changing INH concentrations. In our simulations, we assumed that the same events occurred between INH and *M. tuberculosis* bacilli in the ELF. Also, the experiments by Gumbo et al. (14) were carried out with an avirulent *M. tuberculosis* strain. The effects of INH on virulent strains might well be different.

It is also acknowledged that study data were sparse, especially drug concentrations measured in lungs, as only a single sample obtained 2 h or 4 h after the dose was available for each subject (17, 18). Our model-based estimates of drug AUC and PK profiles in lungs are based on this limited information; therefore, delayed diffusion and accumulation of INH in the ELF cannot be ruled out. However, because INH is a small molecule, with 0% protein binding in plasma, rapid passive transfer from plasma to lungs is expected to occur. To our knowledge, our analysis pooled all pulmonary concentration data for INH that have been published to date.

Data sparseness might raise concerns about the estimableness of population and individual parameter values. Regarding the structural model, the parsimony principle was respected, as the simplest three-compartment structural model was used to describe the three-output system. This model was structurally identifiable, as all inputs and outputs were reachable (48). The shrinkage issue in the Bayesian posterior estimation of individual parameter values was addressed by using a nonparametric population approach in the final parameter estimation. Leary and Chittenden showed that true nonparametric approaches are relatively resilient to the shrinkage effect (49), and such approaches provide richer and less distorted Bayesian posterior distributions than parametric methods (50).

Although we were able to estimate INH concentrations in alveolar cells, the intracellular effects of INH were not investigated in the simulations, because no data on the relationship between intracellular *M. tuberculosis* and intracellular INH exposure has been published to date. Jayaram et al. studied the intracellular killing effect as a function of INH concentrations, although the concentrations were measured in the culture medium and not inside the cells; their results suggested that the intracellular killing effect of INH is almost negligible and has virtually no influence on the EBA (13).

The emergence of INH resistance was not included in our simulations. Gumbo et al. showed that, unlike the bactericidal effect, the relationship between the emergence of resistance and INH exposure could not be described by a simple equation, such as a sigmoidal E_{max} model (14). Emergence appears to be a time-dependent process, which cannot be suppressed after a few days *in vitro*, even with very high levels of INH exposure. Therefore, the best way to prevent the emergence of INH resistance is the optimal use of companion drugs, especially rifampin (51, 52).

To conclude, we have presented the first population model of the pulmonary pharmacokinetics of INH. The results showed that the mean INH exposure in ELF was a little greater than that achieved in plasma, but very large variability was observed. Simulations based on this model and published pharmacodynamic models of INH bactericidal effects against *M. tuberculosis* suggested that patients infected with poorly susceptible *M. tuberculosis* strains, especially FA individuals, may well benefit from higher INH doses, while dose adjustment for acetylator status probably would have little effect on EBA in patients infected with low-MIC organisms.

ACKNOWLEDGMENT

J. E. Conte, Jr., formerly in the Department of Medicine, University of California, San Francisco, is gratefully acknowledged for providing some of the pharmacokinetic data.

REFERENCES

1. **World Health Organization.** 2012. Global burden of disease. World Health Organization, Geneva, Switzerland.
2. **Kimerling ME, Phillips P, Patterson P, Hall M, Robinson CA, Dunlap NE.** 1998. Low serum antimycobacterial drug levels in non-HIV-infected tuberculosis patients. Chest **113:**1178–1183. http://dx.doi.org/10.1378/chest.113.5.1178.
3. **Weiner M, Burman W, Vernon A, Benator D, Peloquin CA, Khan A, Weis S, King B, Shah N, Hodge T, Tuberculosis Trials Consortium.** 2003. Low isoniazid concentrations and outcome of tuberculosis treatment with once-weekly isoniazid and rifapentine. Am J Respir Crit Care Med **167:**1341–1347. http://dx.doi.org/10.1164/rccm.200208-951OC.
4. **Mehta JB, Shantaveerapa H, Byrd RP, Morton SE, Fountain F, Roy TM.** 2001. Utility of rifampin blood levels in the treatment and follow-up of active pulmonary tuberculosis in patients who were slow to respond to routine directly observed therapy. Chest **120:**1520–1524. http://dx.doi.org/10.1378/chest.120.5.1520.
5. **Pasipanodya JG, McIlleron H, Burger A, Wash PA, Smith P, Gumbo T.** 2013. Serum drug concentrations predictive of pulmonary tuberculosis outcomes. J Infect Dis **208:**1464–1473. http://dx.doi.org/10.1093/infdis/jit352.
6. **Jindani A, Doré CJ, Mitchison DA.** 2003. Bactericidal and sterilizing activities of antituberculosis drugs during the first 14 days. Am J Respir Crit Care Med **167:**1348–1354. http://dx.doi.org/10.1164/rccm.200210-1125OC.
7. **de Steenwinkel JEM, de Knegt GJ, ten Kate MT, van Belkum A, Verbrugh HA, Kremer K, van Soolingen D, Bakker-Woudenberg IAJM.** 2010. Time-kill kinetics of anti-tuberculosis drugs, and emergence of resistance, in relation to metabolic activity of *Mycobacterium tuberculosis*. J Antimicrob Chemother **65:**2582–2589. http://dx.doi.org/10.1093/jac/dkq374.
8. **Donald PR, Sirgel FA, Venter A, Parkin DP, Seifart HI, van de Wal BW, Maritz JS, Fourie PB.** 2003. Early bactericidal activity of antituberculosis agents. Expert Rev Anti Infect Ther **1:**141–155. http://dx.doi.org/10.1586/14787210.1.1.141.
9. **Ahmad Z, Klinkenberg LG, Pinn ML, Fraig MM, Peloquin CA, Bishai WR, Nuermberger EL, Grosset JH, Karakousis PC.** 2009. Biphasic kill curve of isoniazid reveals the presence of drug-tolerant, not drug-resistant, *Mycobacterium tuberculosis* in the guinea pig. J Infect Dis **200:**1136–1143. http://dx.doi.org/10.1086/605605.
10. **Gumbo T, Louie A, Liu W, Ambrose PG, Bhavnani SM, Brown D, Drusano GL.** 2007. Isoniazid's bactericidal activity ceases because of the emergence of resistance, not depletion of *Mycobacterium tuberculosis* in the log phase of growth. J Infect Dis **195:**194–201. http://dx.doi.org/10.1086/510247.
11. **Hickman D, Sim E.** 1991. *N*-Acetyltransferase polymorphism: comparison of phenotype and genotype in humans. Biochem Pharmacol **42:**1007–1014. http://dx.doi.org/10.1016/0006-2952(91)90282-A.
12. **Peloquin CA, Jaresko GS, Yong CL, Keung AC, Bulpitt AE, Jelliffe RW.** 1997. Population pharmacokinetic modeling of isoniazid, rifampin, and pyrazinamide. Antimicrob Agents Chemother **41:**2670–2679.
13. **Jayaram R, Shandil RK, Gaonkar S, Kaur P, Suresh BL, Mahesh BN, Jayashree R, Nandi V, Bharath S, Kantharaj E, Balasubramanian V.** 2004. Isoniazid pharmacokinetics-pharmacodynamics in an aerosol infection model of tuberculosis. Antimicrob Agents Chemother **48:**2951–2957. http://dx.doi.org/10.1128/AAC.48.8.2951-2957.2004.
14. **Gumbo T, Louie A, Liu W, Brown D, Ambrose PG, Bhavnani SM, Drusano GL.** 2007. Isoniazid bactericidal activity and resistance emergence: integrating pharmacodynamics and pharmacogenomics to predict efficacy in different ethnic populations. Antimicrob Agents Chemother **51:**2329–2336. http://dx.doi.org/10.1128/AAC.00185-07.
15. **Donald PR, Sirgel FA, Venter A, Parkin DP, Seifart HI, van de Wal BW, Werely C, van Helden PD, Maritz JS.** 2004. The influence of human *N*-acetyltransferase genotype on the early bactericidal activity of isoniazid. Clin Infect Dis **39:**1425–1430. http://dx.doi.org/10.1086/424999.
16. **Kiem S, Schentag JJ.** 2008. Interpretation of antibiotic concentration ratios measured in epithelial lining fluid. Antimicrob Agents Chemother **52:**24–36. http://dx.doi.org/10.1128/AAC.00133-06.
17. **Conte JE, Jr, Golden JA, McQuitty M, Kipps J, Duncan S, McKenna E, Zurlinden E.** 2002. Effects of gender, AIDS, and acetylator status on intrapulmonary concentrations of isoniazid. Antimicrob Agents Chemother **46:**2358–2364. http://dx.doi.org/10.1128/AAC.46.8.2358-2364.2002.
18. **O'Brien JK, Doerfler ME, Harkin TJ, Rom WN.** 1998. Isoniazid levels in the bronchoalveolar lavage fluid of patients with pulmonary tuberculosis. Lung **176:**205–211. http://dx.doi.org/10.1007/PL00007603.
19. **Katiyar SK, Bihari S, Prakash S.** 2008. Low-dose inhaled versus standard dose oral form of anti-tubercular drugs: concentrations in bronchial epithelial lining fluid, alveolar macrophage and serum. J Postgrad Med **54:**245–246. http://dx.doi.org/10.4103/0022-3859.41823.
20. **Grant DM, Tang BK, Kalow W.** 1983. Polymorphic *N*-acetylation of a caffeine metabolite. Clin Pharmacol Ther **33:**355–359. http://dx.doi.org/10.1038/clpt.1983.45.
21. **Delahunty T, Lee B, Conte JE.** 1998. Sensitive liquid chromatographic technique to measure isoniazid in alveolar cells, bronchoalveolar lavage and plasma in HIV-infected patients. J Chromatogr B Biomed Sci Appl **705:**323–329. http://dx.doi.org/10.1016/S0378-4347(97)00510-0.
22. **Rennard SI, Basset G, Lecossier D, O'Donnell KM, Pinkston P, Martin PG, Crystal RG.** 1986. Estimation of volume of epithelial lining fluid recovered by lavage using urea as marker of dilution. J Appl Physiol **60:**532–538.
23. **Gupta RN, Lew M.** 1988. Determination of isoniazid in plasma by liquid chromatography. J Chromatogr B Biomed Sci Appl **425:**441–443. http://dx.doi.org/10.1016/0378-4347(88)80053-7.
24. **Neely MN, van Guilder MG, Yamada WM, Schumitzky A, Jelliffe RW.** 2012. Accurate detection of outliers and subpopulations with Pmetrics, a nonparametric and parametric pharmacometric modeling and simulation package for R. Ther Drug Monit **34:**467–476. http://dx.doi.org/10.1097/FTD.0b013e31825c4ba6.
25. **Tatarinova T, Neely M, Bartroff J, van Guilder M, Yamada W, Bayard D, Jelliffe R, Leary R, Chubatiuk A, Schumitzky A.** 2013. Two general methods for population pharmacokinetic modeling: non-parametric adaptive grid and non-parametric Bayesian. J Pharmacokinet Pharmacodyn **40:**189–199. http://dx.doi.org/10.1007/s10928-013-9302-8.
26. **Goutelle S, Bourguignon L, Bleyzac N, Maire P, Jelliffe RW.** 2009. Performing Monte Carlo simulation based on nonparametric pharmacokinetic parameter distributions: evaluation of various methods applied to a paediatric population study on busulfan, abstr 1525, p 18. Abstr Annu Meet Popul Approach Group Eur.
27. **Schön T, Juréen P, Giske CG, Chryssanthou E, Sturegård E, Werngren J, Kahlmeter G, Hoffner SE, Angeby KA.** 2009. Evaluation of wild-type MIC distributions as a tool for determination of clinical breakpoints for *Mycobacterium tuberculosis*. J Antimicrob Chemother **64:**786–793. http://dx.doi.org/10.1093/jac/dkp262.
28. **Gumbo T.** 2010. New susceptibility breakpoints for first-line antituberculosis drugs based on antimicrobial pharmacokinetic/pharmacodynamic science and population pharmacokinetic variability. Antimicrob Agents Chemother **54:**1484–1491. http://dx.doi.org/10.1128/AAC.01474-09.
29. **Centers for Disease Control and Prevention.** 2012. *Mycobacterium tuberculosis*: drug susceptibility testing program. Centers for Disease Control and Prevention, Atlanta, GA.
30. **Kinzig-Schippers M, Tomalik-Scharte D, Jetter A, Scheidel B, Jakob V, Rodamer M, Cascorbi I, Doroshyenko O, Sörgel F, Fuhr U.** 2005. Should we use *N*-acetyltransferase type 2 genotyping to personalize isoniazid doses? Antimicrob Agents Chemother **49:**1733–1738. http://dx.doi.org/10.1128/AAC.49.5.1733-1738.2005.
31. **Wilkins JJ, Langdon G, McIlleron H, Pillai G, Smith PJ, Simonsson USH.** 2011. Variability in the population pharmacokinetics of isoniazid in South African tuberculosis patients. Br J Clin Pharmacol **72:**51–62. http://dx.doi.org/10.1111/j.1365-2125.2011.03940.x.
32. **Donald PR, Parkin DP, Seifart HI, Schaaf HS, van Helden PD, Werely CJ, Sirgel FA, Venter A, Maritz JS.** 2007. The influence of dose and *N*-acetyltransferase-2 (NAT2) genotype and phenotype on the pharmacokinetics and pharmacodynamics of isoniazid. Eur J Clin Pharmacol **63:**633–639. http://dx.doi.org/10.1007/s00228-007-0305-5.
33. **Peloquin CA, Namdar R, Dodge AA, Nix DE.** 1999. Pharmacokinetics of isoniazid under fasting conditions, with food, and with antacids. Int J Tuberc Lung Dis **3:**703–710.
34. **Sahin S, Benet LZ.** 2008. The operational multiple dosing half-life: a key to defining drug accumulation in patients and to designing extended re-

lease dosage forms. Pharm Res **25:**2869–2877. http://dx.doi.org/10.1007/s11095-008-9787-9.

35. **Wagner JG.** 1976. Linear pharmacokinetic equations allowing direct calculation of many needed pharmacokinetic parameters from the coefficients and exponents of polyexponential equations which have been fitted to the data. J Pharmacokinet Biopharm **4:**443–467. http://dx.doi.org/10.1007/BF01062831.
36. **Bhatt NB, Barau C, Amin A, Baudin E, Meggi B, Silva C, Furlan V, Grinsztejn B, Barrail-Tran A, Bonnet M, Taburet AM.** 2014. Pharmacokinetics of rifampin and isoniazid in tuberculosis-HIV-coinfected patients receiving nevirapine- or efavirenz-based antiretroviral treatment. Antimicrob Agents Chemother **58:**3182–3190. http://dx.doi.org/10.1128/AAC.02379-13.
37. **Lin M-Y, Lin S-J, Chan L-C, Lu Y-C.** 2010. Impact of food and antacids on the pharmacokinetics of anti-tuberculosis drugs: systematic review and meta-analysis. Int J Tuberc Lung Dis **14:**806–818.
38. **Donald PR, Sirgel FA, Botha FJ, Seifart HI, Parkin DP, Vandenplas ML, Van de Wal BW, Maritz JS, Mitchison DA.** 1997. The early bactericidal activity of isoniazid related to its dose size in pulmonary tuberculosis. Am J Respir Crit Care Med **156:**895–900. http://dx.doi.org/10.1164/ajrccm.156.3.9609132.
39. **Pasipanodya JG, Srivastava S, Gumbo T.** 2012. Meta-analysis of clinical studies supports the pharmacokinetic variability hypothesis for acquired drug resistance and failure of antituberculosis therapy. Clin Infect Dis **55:**169–177. http://dx.doi.org/10.1093/cid/cis353.
40. **Donald PR, Diacon AH.** 2008. The early bactericidal activity of antituberculosis drugs: a literature review. Tuberculosis **88**(Suppl 1)**:**S75–S83. http://dx.doi.org/10.1016/S1472-9792(08)70038-6.
41. **Sirgel FA, Donald PR, Odhiambo J, Githui W, Umapathy KC, Paramasivan CN, Tam CM, Kam KM, Lam CW, Sole KM, Mitchison DA.** 2000. A multicentre study of the early bactericidal activity of antituberculosis drugs. J Antimicrob Chemother **45:**859–870. http://dx.doi.org/10.1093/jac/45.6.859.
42. **Gumbo T, Pasipanodya JG, Wash P, Burger A, McIlleron H.** 2014. Redefining multidrug-resistant tuberculosis based on clinical response to combination therapy. Antimicrob Agents Chemother **58:**6111–6115. http://dx.doi.org/10.1128/AAC.03549-14.
43. **World Health Organization Stop TB Initiative.** 2010. Treatment of tuberculosis: guidelines, 4th ed. World Health Organization, Geneva, Switzerland.
44. **Katiyar SK, Bihari S, Prakash S, Mamtani M, Kulkarni H.** 2008. A randomised controlled trial of high-dose isoniazid adjuvant therapy for multidrug-resistant tuberculosis. Int J Tuberc Lung Dis **12:**139–145.
45. **Kass JS, Shandera WX.** 2010. Nervous system effects of antituberculosis therapy. CNS Drugs **24:**655–667. http://dx.doi.org/10.2165/11534340-000000000-00000.
46. **Aouam K, Chaabane A, Loussaïef C, Ben Romdhane F, Boughattas N-A, Chakroun M.** 2007. Adverse effects of antitubercular drugs: epidemiology, mechanisms, and patient management. Med Mal Infect **37:**253–261. (In French.) http://dx.doi.org/10.1016/j.medmal.2006.12.006.
47. **Dartois V.** 2014. The path of anti-tuberculosis drugs: from blood to lesions to mycobacterial cells. Nat Rev Microbiol **12:**159–167. http://dx.doi.org/10.1038/nrmicro3200.
48. **Bonate PL.** 2005. Pharmacokinetic-pharmacodynamic modeling and simulation. Springer, New York, NY.
49. **Leary R, Chittenden J.** 2008. A nonparametric analogue to POSTHOC estimates for exploratory data analysis, abstr 1343, p 17. Abstr Annu Meet Popul Approach Group Eur.
50. **de Hoog M, Schoemaker RC, van den Anker JN, Vinks AA.** 2002. NONMEM and NPEM2 population modeling: a comparison using tobramycin data in neonates. Ther Drug Monit **24:**359–365. http://dx.doi.org/10.1097/00007691-200206000-00006.
51. **Gumbo T, Louie A, Deziel MR, Liu W, Parsons LM, Salfinger M, Drusano GL.** 2007. Concentration-dependent *Mycobacterium tuberculosis* killing and prevention of resistance by rifampin. Antimicrob Agents Chemother **51:**3781–3788. http://dx.doi.org/10.1128/AAC.01533-06.
52. **Goutelle S, Bourguignon L, Maire PH, Van Guilder M, Conte JE, Jelliffe RW.** 2009. Population modeling and Monte Carlo simulation study of the pharmacokinetics and antituberculosis pharmacodynamics of rifampin in lungs. Antimicrob Agents Chemother **53:**2974–2981. http://dx.doi.org/10.1128/AAC.01520-08.